

## Kinetics study and influence of water-soluble polymer on the electrodeposition of iron from a citrate-chloride electrolyte on the basis of Fe(III)

Vyacheslav PROTSENKO\*, Felix DANILOV

Ukrainian State University of Chemical Technology, Dnepropetrovsk, Ukraine

Received: 24.09.2014

Accepted/Published Online: 08.12.2014

Printed: 30.06.2015

**Abstract:** The kinetics of the iron electrodeposition reaction from a plating bath containing trivalent iron ions is investigated in the present work. The electrochemical reaction is stated to proceed via the formation of relatively stable intermediates: Fe(II) ions. Only a part of the total amount of Fe(II) ions formed at the first stage of Fe(III) discharge is reduced further, producing metal iron. The effect of polyhexamethyleneguanidine hydrochloride (with an average molecular weight of 1000) on the iron deposition is ascertained. The presence of polymer additive in the iron electrolyte appreciably affects the rate of iron deposition, while the polymer additive does not influence the rate of Fe(III) ions discharge. The effect of polyhexamethyleneguanidine on the rate of iron electrodeposition is discussed in terms of the influence of the oligomer on the aggregative stability of the  $\text{Fe}(\text{OH})_3$  sol formed in the near-electrode layer.

**Key words:** Electroplating, iron, kinetics, polyhexamethyleneguanidine, polarization curve, aggregative stability

### 1. Introduction

The electrodeposition of iron and its alloys has been widely used for various engineering applications such as electroforming, electrotypes, repairing worn and corroded machine parts, magnetics components in computer and electronic industries, and microelectromechanical systems.<sup>1–5</sup> Iron electrodeposits are usually obtained from acidic sulfate, chloride, fluoroborate, and sulfamate Fe(II) electrolytes, although weak-acid Fe(III) baths have also been reported.<sup>6–8</sup> Acidic iron electroplating baths containing Fe(II) salts are well studied; they are highly productive and easily manageable. Nevertheless, acidic electrolytes for iron electrodeposition are rather corrosive and toxic; they cannot be directly used in the electroplating of zinc alloys, pig iron, and various light metals that corrode intensively in acid solutions. Therefore, the development of novel iron electroplating baths is an important problem of modern electroplating. Earlier<sup>7,8</sup> an iron bath was proposed that contains  $\text{FeCl}_3$ ,  $\text{Na}_3\text{Cit}$  (sodium citrate),  $\text{NaCl}$ , and  $\text{H}_3\text{BO}_3$ ; it is operated at  $\text{pH} \sim 5$  and temperature of about 20–30 °C. Due to the low acidity of the solution and medium electrodeposition temperature, the electrolyte involved has no a strong etching effect on various materials. Therefore, the iron coatings obtained from this plating bath could be used as interlayers in the electrodeposition of different coatings on the surfaces of metals that are readily soluble in aggressive medium. For instance, the citrate-chloride electrolyte on the basis of Fe(III) was shown to be applied for obtaining an iron intermediate layer on the zinc deposit surface before chromium electroplating.<sup>7</sup>

To date, reports on the regularities of iron electrodeposition from Fe(III)-containing baths have been very limited.<sup>6–8</sup> The kinetics of metal deposition reaction as well as the influence of bath constituents is yet to be

\*Correspondence: [vprotsenko7@gmail.com](mailto:vprotsenko7@gmail.com)

fully rationalized. Thus, organic additives were shown to play an important role in iron electroplating.<sup>4</sup> Organic additives affect the polarization curves of metals and can improve surface characteristics such as brightness, leveling, and anticorrosion properties.

Among organic additives, special attention has been paid to water-soluble polymers, and their beneficial effects on the electrodeposition processes of various metals were recently established in a number of works.<sup>9–13</sup> However, the influence of polymer additives on iron electrochemical deposition has not been described yet. In this paper, we aim to understand, in particular, the effect of a water-soluble polymer on the iron deposition process from the electrolyte on the basis of Fe(III) salts.

## 2. Results

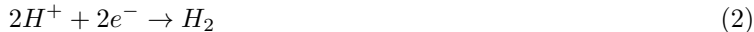
### 2.1. Kinetics of electrode processes occurring during iron deposition from a citrate-chloride bath

Stationary partial polarization curves were obtained in order to identify the electrochemical reactions proceeding at the cathode in the bath under consideration (Figure 1). As can be seen, the main electrode process is a reduction of Fe(III) when electrode potentials are more positive than  $-0.8$  V:



No cathode mass gain and no hydrogen evolution were detected in this range of electrode potential. Reaction (1) seems to proceed under the conditions of limiting diffusion current.

A hydrogen evolution reaction (HER) with an appreciable rate can be observed at  $E < -0.8$  V:



This process is characterized by a typical exponential polarization curve. Obviously, an agitation of the near-electrode layer by hydrogen bubbles evolved leads to diminishing effective thickness of the diffusion layer.<sup>14</sup> As a result, the limiting diffusion current of reaction (1) increases somewhat when the HER starts.

Electrodeposition of iron (Eq. (6)) from the electrolyte under study begins when electrode potential reaches the cathodic value of about  $-0.9$  V (Figure 1, curve 2), i.e. under the conditions of the limiting diffusion current of reaction (1).



It should be observed that a plateau of the limiting current of iron deposition appears at cathode potentials  $E < -1.2$  V.

As shown in our previous work,<sup>15</sup> the effect of the diffusion mass transfer intensity on the rates of individual stages in consecutive electrochemical reactions may serve as their diagnostic criterion. Therefore, we investigated the influence of electrolyte stirring on the kinetics of partial electrochemical processes. Figure 2 shows the effect of electrolyte agitation by a magnetic stirrer (60 rpm) on the partial polarization curves of electrode processes (1), (2), and (3).

Electrolyte stirring leads to an increase in the current density of Fe(III) ions discharge, which confirms the convection-diffusion limitations of this reaction (Figure 2a).

In the initial segment of the polarization curve, the rate of the iron deposition reaction decreases in a stirred solution (Figure 2b). In contrast, the limiting current of metal electrodeposition (i.e. the current plateau in the polarization curve) grows if the electrolyte is stirred. As expected, the current of the HER does

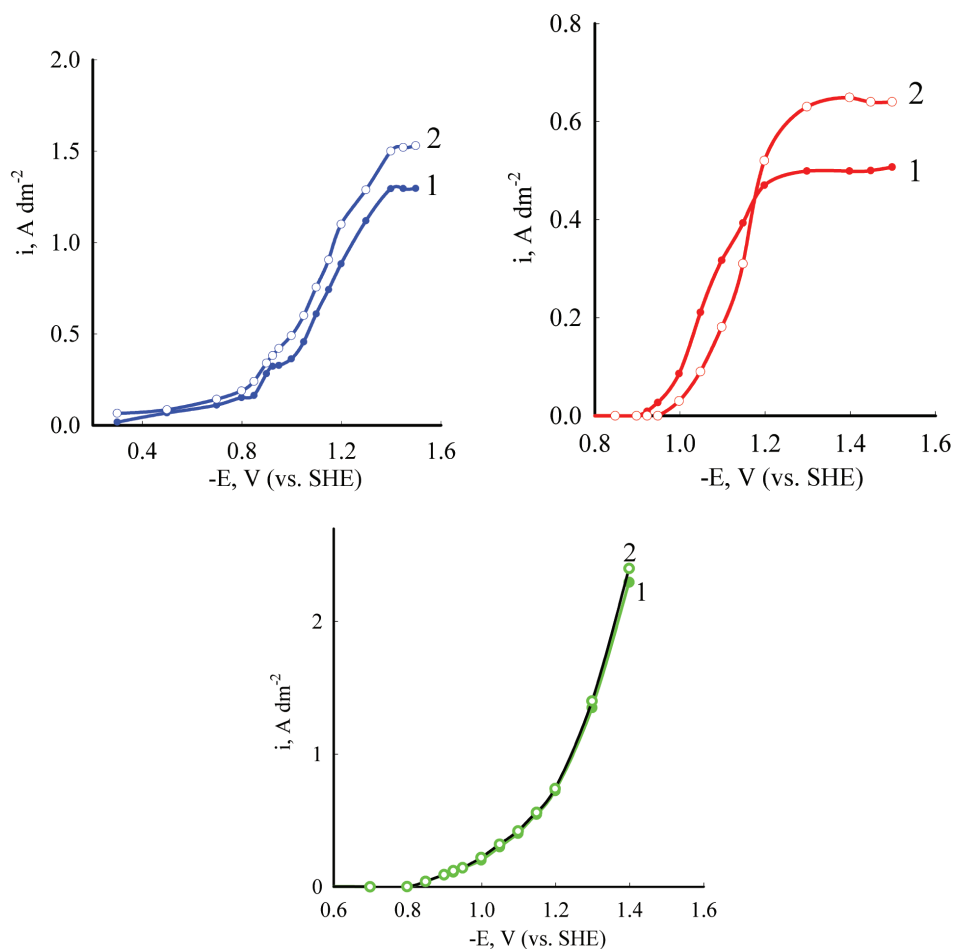


**Figure 1.** Steady-state partial polarization curves for electrochemical reaction: (1)  $\text{Fe(III)} + e^- \rightarrow \text{Fe(II)}$ , (2)  $\text{Fe(II)} + 2e^- \rightarrow \text{Fe(0)}$ , (3)  $2\text{H}^+ + 2e^- \rightarrow \text{H}_2$ . Curve 4 presents the overall (total) polarization current. The electrolyte contains 0.05 M  $\text{FeCl}_3$ , 0.2 M  $\text{Na}_3\text{Cit}$ , 0.5 M  $\text{NaCl}$ , and 0.5 M  $\text{H}_3\text{BO}_3$ ; pH 5.

not depend on the electrolyte agitation since this electrochemical reaction is well known to be controlled by the slow charge transfer (Figure 2c).

## 2.2. Effect of water-soluble polymer on iron electrodeposition

In the present work, we investigate the effect of polyhexamethyleneguanidine hydrochloride (PHMG) on the electrochemical reactions occurring during iron deposition in the citrate-chloride electrolyte under consideration. PHMG is a cationic polymer in aqueous media; its chemical structure is presented in Figure 3. PHMG has attracted considerable attention for its high antibacterial activity and low toxicity to humans; it has been extensively used in anti-infective solutions in medicine and as disinfectants and biocides.<sup>16</sup> The average molecular weight of the PHMG used in the present work was about 1000.

Figure 4 demonstrates cyclic voltammograms obtained on a graphite electrode. As shown in our previous work,<sup>8</sup> the cathodic and anodic waves recorded on a graphite electrode at  $-0.1$  and  $+0.2$  V, respectively, correspond to the irreversible reaction (1). At the potentials  $E < -0.9$  V there occurs discharge of  $\text{Fe(II)}$  (i.e. reaction (3)), which is accompanied by the hydrogen evolution reaction. The anodic current wave at  $E \sim -0.4$  V corresponds to the dissolution of iron deposited in a foregoing cathodic scan. It is obviously that the

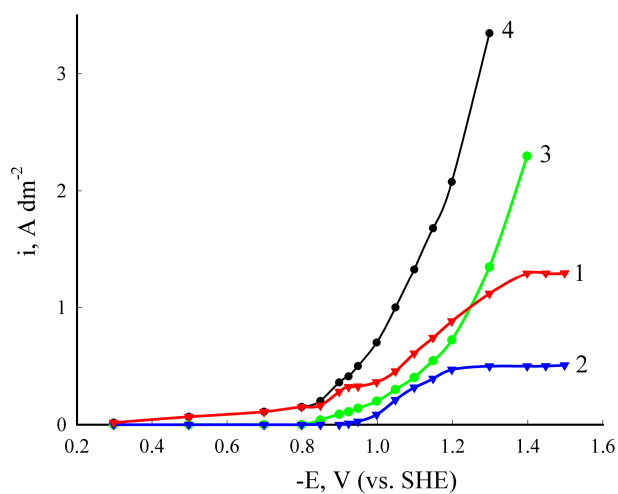


**Figure 2.** Steady-state partial polarization curves for electrochemical reaction: (a)  $\text{Fe(III)} + e^- \rightarrow \text{Fe(II)}$ , (b)  $\text{Fe(II)} + 2e^- \rightarrow \text{Fe(0)}$ , (c)  $2\text{H}^+ + 2e^- \rightarrow \text{H}_2$ . (1) unstirred electrolyte, (2) stirring by a magnetic stirrer. The electrolyte contains 0.05 M  $\text{FeCl}_3$ , 0.2 M  $\text{Na}_3\text{Cit}$ , 0.5 M  $\text{NaCl}$ , and 0.5 M  $\text{H}_3\text{BO}_3$ ; pH 5.

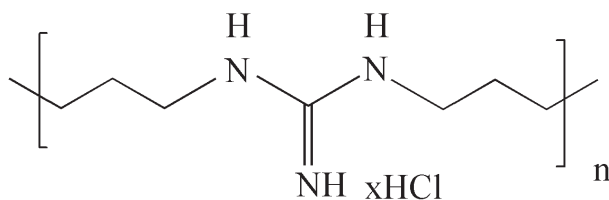


**Figure 3.** Chemical structure of PHMG in cationic form.

charge consumed in the iron deposition reaction is equal to the charge spent for the anodic dissolution of iron. Therefore, the area under the anodic current wave at  $E \sim -0.4$  V is directly proportional to the amount of deposited iron.

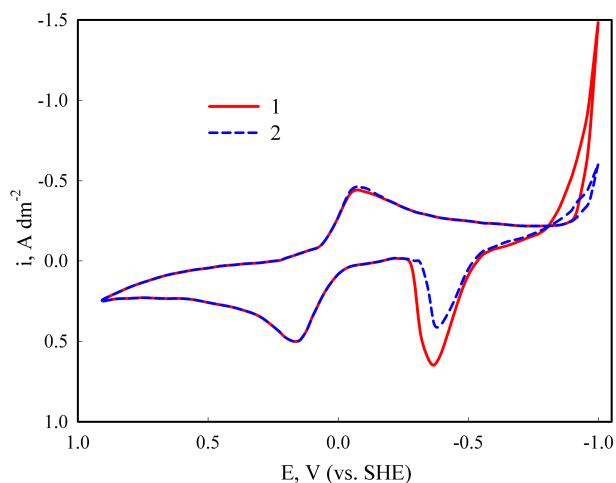


**Figure 4.** Cyclic voltammograms obtained on a graphite electrode in basic citrate-chloride bath (1) without polymers additive and (2) with the addition of  $1 \times 10^{-4}$  M PHMG. Scan rate  $50 \text{ mV s}^{-1}$ .

As can be seen, the presence of PHMG in the iron electrolyte does not affect the rate of electrochemical reaction (1). Meanwhile, the introduction of PHMG into the solution causes shifting of the wave of metal deposition towards more negative potentials as well as diminishing the area under the anodic current wave of iron dissolution. This indicates the deceleration of the iron electrodeposition reaction.

In order to acquire more detailed information on the influence of polymer additive on the kinetics of metal deposition, steady-state partial polarization curves were obtained at different content of PHMG (Figure 5).

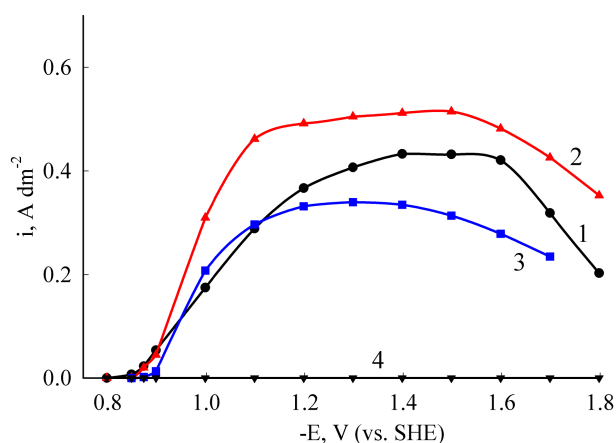


**Figure 5.** Partial polarization curves of iron deposition obtained in basic citrate-chloride bath without polymer additive (1) and with the addition of  $1 \times 10^{-6}$  M PHMG (2),  $1 \times 10^{-5}$  M PHMG (3),  $1 \times 10^{-4}$  M PHMG (4). Curve (4) practically coincides with the abscissa axis.

The addition of PHMG to an iron plating bath has a strong effect on the rate of metal electrodeposition. In the initial (ascending) segment of the polarization curve, the rate of iron deposition decreases somewhat with an increase in the polymer content, whereas the influence of PHMG upon the iron electrodeposition rate is nonmonotonic in the potentials range relating to the current plateau (Figure 5). Thus, at a low content of PHMG ( $1 \times 10^{-6}$  M), the partial current increases; however, at a higher content ( $1 \times 10^{-5}$  M), the Fe deposition rate is even less than in electrolyte without polymer additive.

To explain such a complicated influence, one should take into account that the emergence of current plateaus in partial polarization curves may be associated with the formation of poorly soluble hydroxides in the near-electrode layer.<sup>8</sup> Evidently, polyhexamethyleneguanidine can appreciably affect the structure and aggregative stability of the  $\text{Fe}(\text{OH})_3$  sol in the near-electrode layer and thereby strongly influence the kinetics of electrode processes.

To verify this assumption, we carried out a turbidimetric study of the aggregative stability of the  $\text{Fe}(\text{OH})_3$  sol in the presence of the PHMG additive. The  $\text{Fe}(\text{OH})_3$  sol was prepared in laboratory conditions. The preparation procedure is described in the Experimental section. The time dependences of the absorbance of the sol are represented as curves with a maximum (Figure 6). We will consider these dependences in the Discussion section.

### 3. Discussion

Previously<sup>8</sup> we stated that the iron electrodeposition from citrate-chloride electrolytes containing Fe(III) proceeds stepwise via the formation of relatively stable intermediates: Fe(II) ions. Such behavior results from a

considerable difference between the standard electrode potentials of reactions (1) and (3); iron deposition should start at potentials that are more negative than those of incomplete reduction (1). The kinetics of consecutive electrochemical reactions with the participation of relatively stable intermediates has been discussed in our previous works.<sup>15,17</sup> In accordance with the developed formalism, the following equation reflecting the condition of material balance of the intermediates should be valid under the quasisteady-state conditions:

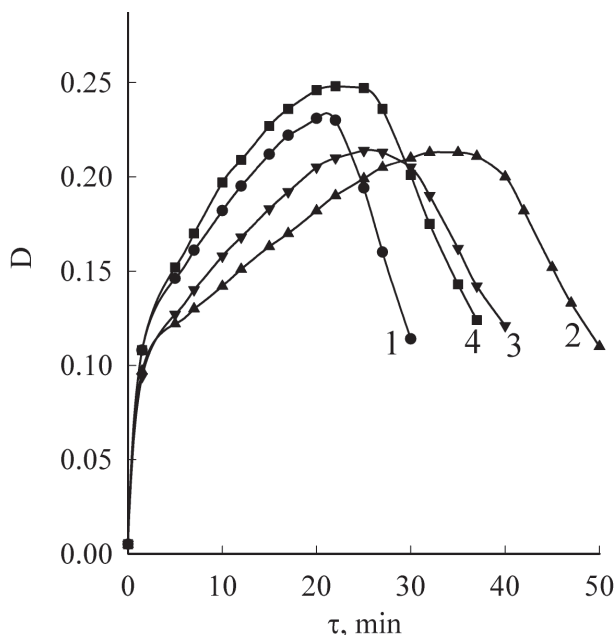


**Figure 6.** Time dependence of the absorbance of  $\text{Fe}(\text{OH})_3$  sol: (1) without PHMG, and with the addition of  $1 \times 10^{-6}$  M PHMG (2),  $1 \times 10^{-5}$  M PHMG (3),  $1 \times 10^{-4}$  M PHMG (4).

$$\frac{i_{\text{Fe(III)} \rightarrow \text{Fe(II)}}}{F} = \frac{i_{\text{Fe(II)} \rightarrow \text{Fe(0)}}}{2F} + \nu, \quad (4)$$

where  $i_{\text{Fe(III)} \rightarrow \text{Fe(II)}}$  and  $i_{\text{Fe(II)} \rightarrow \text{Fe(0)}}$  are the partial currents of the corresponding reactions;  $\nu$  is the rate of the convective-diffusion flow of intermediates between electrode surface and bulk solution.

Since we did not accumulate  $\text{Fe(II)}$  ions before the electrodeposition experiments, the content of bivalent iron ions in bulk solution is practically zero. Then the content of intermediates (i.e.  $\text{Fe(II)}$  ions) near the electrode surface is sufficiently higher than that in the bulk electrolyte; therefore, the flow is directed from the electrode to the bulk electrolyte and  $\nu \geq 0$ . Taking into account the last inequality, the following relationship may be easily derived from (4):

$$2i_{\text{Fe(III)} \rightarrow \text{Fe(II)}} \geq i_{\text{Fe(II)} \rightarrow \text{Fe(0)}}. \quad (5)$$

Analysis of the experimental results shows that the condition (5) is fulfilled for all values of electrode potential where metal iron deposits on the cathode. It means that only a part of the total amount of  $\text{Fe(II)}$  ions formed at the first stage of  $\text{Fe(III)}$  discharge is reduced further, producing metal iron. The excess of bivalent iron ions is removed to the bulk electrolyte.

As shown above (Figure 2b), the rate of the Fe electrodeposition process in the initial (ascending) segment of the polarization curve diminishes when a solution is stirred. According to the theoretical approach developed in previous works,<sup>8,15,17</sup> such behavior is accounted for by an intensification of partial removal of intermediates

to the bulk electrolyte under the condition of enhanced convective mass transfer. As a result, the surface concentration of Fe(II) ions diminishes and the rate of reaction (3) evidently decreases.

If we assume that the plateau of limiting current of iron deposition in the partial polarization curve is caused by the convection-diffusion limitations of the transport of Fe(III) ions, then the Fe(II) ions formed in reaction (1) should be completely consumed in reaction (3) and the following equalities might be valid:  $\nu = 0$  and  $i_{Fe(II) \rightarrow Fe(0)} = 2i_{Fe(III) \rightarrow Fe(II)}$ . However, these conditions are not fulfilled at the potentials of limiting current of iron deposition. Thus bivalent iron ions are not spent fully in the reaction of Fe(II) discharge to metal and diffuse, in part, into the bulk electrolyte. Therefore, the formation of the limiting current plateau in the  $i, E$  – curve of metal deposition seems not to be connected with any diffusion restrictions on the transport of iron ions. However, in accordance with the experimental results, the value of the limiting current of iron electroplating increases in a stirred electrolyte. In order to clarify these phenomena, one should take into account that the HER occurs at the cathode simultaneously with the metal electrodeposition. The acceleration of the HER with increasing cathodic polarization leads to an increase in the pH value in the near electrode layer (i.e.  $pH_S$ ), and, consequently, to the formation of poorly soluble hydroxide compounds of Fe(III) there.<sup>8</sup> As a result, the reaction of iron deposition should decelerate. Additionally, hydroxide compounds of trivalent iron adsorb on the electrode surface and block it. In a certain potential region, this inhibition effect may approximately counterbalance the accelerating action of the electric field and give rise to the plateau in the polarization curve. Such argumentation<sup>17,18</sup> was used earlier to explain the reasons for appearance of limiting current plateaus during chromium deposition in trivalent chromium baths.

The blocking of the electrode surface by poorly soluble Fe(III) hydroxide compounds must be highly sensitive to changes in the convective mass transfer, which agrees well with our data. Indeed, the  $pH_S$  value and the cathode blocking by adsorbed Fe(III) hydroxide evidently decrease when the electrolyte is stirred.

In addition, the processes of colloidal particles aggregation in the near-electrode layer, and, therefore, cathode blocking should be affected to a considerable degree by the introduction of water-soluble polymers into the plating bath.<sup>11,12</sup> The obtained data confirm this assumption.

Indeed, as can be seen from Figure 5, the iron electrodeposition process decelerates with an increase in the PHMG content in the initial section of the polarization curves. This may be explained by the adsorption of cationic polyelectrolyte on the iron surface, which is negatively charged (the zero-charge potential of iron is close to  $-0.37$  V).<sup>19</sup> When the PHMG content in the electrolyte reaches  $1 \times 10^{-4}$  M, the adsorption layer on the cathode is so strong that the iron deposition does not occur at all (in the investigated potential range). At the same time, as stated above, the addition of PHMG has no effect on the kinetics of reaction (1) since this process proceeds on the graphite electrode surface that has no significant negative charge (the zero-charge potential of graphite is about  $-0.07$  V)<sup>19</sup> and, therefore, cationic polyelectrolyte could hardly adsorb on the surface.

The complex (nonmonotonic) effect of polymer concentration on the Fe deposition rate in the potentials range of the current plateau can be associated with the influence of PHMG upon the aggregative stability of the sol formed in the cathode layer during electroplating. This is well correlated with the results of the turbidimetric investigation presented in Figure 6.

A specific extremal view of  $D$  vs. time curves can be elucidated on the basis of the following well-known equation:<sup>20</sup>

$$D = k\nu V^2, \quad (6)$$

where  $D$  is the value of the sol absorbance,  $\nu$  is the particle concentration in the dispersed system,  $V$  is the average particle volume, and  $k$  is a certain constant.

The bell shape of the  $D$  vs. time curve can be associated with the processes of coagulation and subsequent sedimentation of the dispersed phase, which occur in time.<sup>11</sup> The coagulation and flocculation of the particles lead to an increase in particle size (i.e. value  $V$  increases) and to the respective increase in sol absorbance (an ascending segment in  $D$ ,  $\tau$  curves). In the course of particles' coarsening, their sedimentation begins and the phases of the colloidal system are separated, which is easily observed with the unaided eye (a descending segment in  $D$ ,  $\tau$  curves).

Thus, the acceleration of particles' coarsening will result in an increase in sol absorbance in the ascending segment of the  $D$ ,  $\tau$  curve and in a decrease in the absorbance in the descending segment. Additionally, the descending segment in the  $D$ ,  $\tau$  curve appears later if the colloidal system is more stable.

As follows from our findings, the stabilization of  $\text{Fe}(\text{OH})_3$  sol is observed at the lowest content of PHMG in solution ( $1 \times 10^{-6}$  M). At higher polymer content, the aggregative stability of the sol is reduced.

The stabilization of the sol at low polymer content in electrolyte is presumably caused by a "barrier-layer effect". This effect implies that the polymeric molecules or ions form a protective adsorption layer by adsorbing on the  $\text{Fe}(\text{OH})_3$  colloidal particles. The presence of such a protective adsorption layer impedes the interaction between the sol particles, hinders their agglomeration (i.e. coagulation or flocculation), and weakens particle adhesion.

A decrease in the aggregative stability of the  $\text{Fe}(\text{OH})_3$  sol at higher PHMG concentrations may be connected with the adsorptive flocculation, which means that the particles are merged as a result of their adsorption on different segments of a chain macromolecule.

Based on the comparison between the data presented in Figures 5 and 6, we concluded that the growth of the aggregative stability of the sol leads to an increase in the partial current density of iron electrodeposition (a current plateau in the polarization curve) due to the weakening of surface blocking by particles of poorly soluble hydroxide. When the rate of aggregation accelerates, the growing particles block the cathode surface and the current of iron plating diminishes. In addition, at high concentrations of polymer additive, its adsorption on the electrode also promotes the inhibition of the metal electrodeposition reaction.

The introduction of PHMG additive into the iron electrolyte changes the surface appearance of deposits obtained: they become darker with specific tints of glassed marble. Figure 7 gives the surface morphology of the iron coatings. As can be seen, the surface is rather smooth and contains a large number of poorly structured grains (Figure 7a). The addition of polymer additive leads to an appreciable decrease in grain size (Figure 7b). Apparently the adsorption of polymer additive on the electrode surface inhibits the grains' growth.<sup>21</sup>

#### 4. Conclusion

The electrodeposition of iron from a citric-chloride plating bath containing trivalent iron ions occurs as a consecutive electrochemical reaction with the participation of relatively stable intermediates:  $\text{Fe}(\text{II})$  ions. The introduction of polyhexamethyleneguanidine hydrochloride into the iron plating bath affects the aggregative stability of the  $\text{Fe}(\text{OH})_3$  sol formed during metal deposition in the near-electrode layer, and, hence, the rate of electrochemical reactions involved. In the initial segment of the polarization curve, the rate of Fe electrodeposition decreases with an increase in the polymer additive content, whereas the influence of PHMG on the Fe deposition rate is nonmonotonic in the potentials range of the current plateau. At a relatively low content of PHMG ( $1 \times 10^{-6}$  M), the partial current increases; at a higher content ( $1 \times 10^{-5}$  M), the Fe



deposition rate is even less than that in electrolyte without polymer additive. The addition of polymer results in a decrease in grain size.

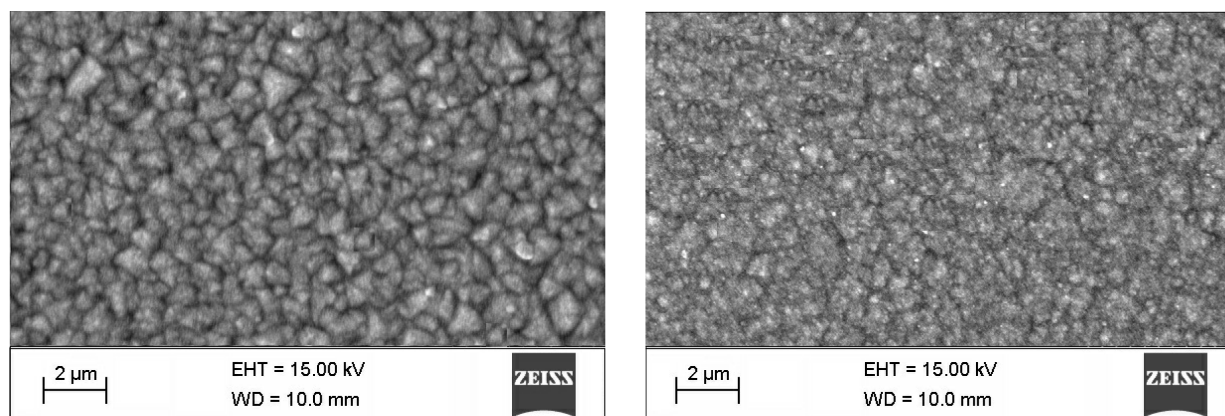


**Figure 7.** SEM images of surface morphology of the iron deposits obtained from the plating bath (a) without polymer additive and (b) with the addition of  $1 \times 10^{-6}$  M PHMG. Current density  $2 \text{ A dm}^{-2}$ , deposits thickness  $1 \mu\text{m}$ .

## 5. Experimental

Iron electrodeposition was performed in the following basic citrate-chloride bath<sup>7,8</sup> ( $\text{mol L}^{-1}$ ):  $0.05 \text{ FeCl}_3$ ,  $0.2 \text{ Na}_3\text{Cit}$ ,  $0.5 \text{ NaCl}$ , and  $0.5 \text{ H}_3\text{BO}_3$ ; pH 5. Iron(III) chloride acts as a metal ions source; sodium citrate plays the role of complexing agent; sodium chloride and boric acid are conducting salt and buffer agent, respectively.

The electrochemical polarization measurements were conducted in a common three-electrode glass cell (250 mL). The solutions were deaerated by blowing with electrolytic hydrogen. The electrochemical cell was thermostated at  $25 \pm 0.1 \text{ }^\circ\text{C}$ .

Steady-state polarization curves were obtained using a stationary copper-foil disc placed in a Plexiglas cartridge with a diameter of 7 mm as the working electrode. Before each experiment, the working electrode was subjected to cathode degreasing in an alkaline solution, activated in a HCl solution (1:1 vol %), then thoroughly washed with distilled water, and dried.

For obtaining cyclic voltammetry curves, an end face of a graphite cylinder ( $0.64 \text{ cm}^2$ ) was employed as the working electrode. The side surface of the cylinder was insulated by an acid-resistant lacquer. Before performing each voltammetric experiment, the working electrode was kept in a HCl solution for 30 s and then thoroughly rinsed with distilled water.

The counter electrode was a large platinum foil; it was separated from a compartment of the working electrode by a glass porous diaphragm. A Ag/AgCl/Sat. KCl electrode was used as a reference electrode through a Luggin probe salt bridge. The potentials were recalculated to a standard hydrogen electrode (SHE) scale.

The working electrode potential was controlled by a Potentiostat/Galvanostat Reference 3000 (Gamry) coupled to a personal computer using support software that allows experimental control and data acquisition. The ohmic potential drop was measured and automatically compensated for by means of the built-in IR-compensator of the potentiostat.

The total current density through the electrochemical cell was determined automatically by means of the potentiostat software. The partial current density of the iron deposition process was calculated from the cathode gain in weight for a deposition time of 20 min. The partial current density of the hydrogen evolution reaction

was found from the hydrogen volume evolved, the hydrogen volume being recalculated for normal conditions and with a correction for the presence of saturated water vapor at the temperature of the experiment.

The polyhexamethyleneguanidine hydrochloride (99.5%) was synthesized at the Institute of Petrochemical Synthesis, RAS.

The effect of water-soluble polymer on the aggregative stability of the  $\text{Fe}(\text{OH})_3$  sol was studied by turbidimetric analysis. To this end, the required amount of polymer additive was added to the 5-times diluted basic iron plating electrolyte, and then the  $\text{Fe}(\text{OH})_3$  sol was manufactured by adding some portions of 1 M NaOH in order to reach the pH value of 10.5. The absorbance of the sol synthesized was measured by means of a photoelectric colorimeter, KFK-2-UkhL-42, directly after sol preparation (the cell thickness was 1 mm, the wavelength was 750 nm, the reference liquid was distilled water).

The morphology of the deposits was investigated by scanning electron microscopy (EVO 40XVP). The samples used in the SEM study were electroplated on electropolished Cu-substrate.

### References

1. Panayotova, M. *Surf. Coat. Technol.* **2000**, *124*, 266–271.
2. Izaki, M.; Miyamoto, N.; Nakae, A.; Hasegawa, T.; Watase, S.; Chigane, M.; Fujiwara, Y.; Ishikawa, M.; Enomoto, H. *J. Electrochem. Soc.* **2002**, *149*, C370–C374.
3. Bai, A.; Hu, C.-C.; Wen, T.-C. *Electrochim. Acta* **2003**, *48*, 2425–2434.
4. Lallemand, F.; Ricq, L.; Wery, M.; Berçot, P.; Pagetti, J. *Appl. Surf. Sci.* **2004**, *228*, 326–333.
5. Péter, L.; Csik, A.; Vad, K.; Tóth-Kádár, E.; Pekker, Á.; Molnár, G. *Electrochim. Acta* **2010**, *55*, 4734–4741.
6. Kuznetsov, V. V.; Golyanin, K. E.; Pshenichkina, T. V.; Lyakhov, B. F.; Lyashenko, S. E. *Mendeleev Commun.* **2013**, *23*, 331–333.
7. Protsenko, V. S.; Danilov, F. I. *Metal Finishing* **2010**, *108*, 28–32.
8. Danilov, F. I.; Protsenko, V. S.; Ubiikon', A. V. *Russ. J. Electrochem.* **2005**, *41*, 1282–1289.
9. Phuong, N. V.; Kwon, S.-C.; Lee, J.-Y.; Shin, J.; Huy, B. T.; Lee Y.-I. *Microchem. J.* **2011**, *99*, 7–14.
10. Phuong, N. V.; Kwon, S. C.; Lee, J. Y.; Lee, J. H.; Lee, K. H. *Surf. Coat. Technol.* **2012**, *206*, 4349–4355.
11. Protsenko, V.; Gordiienko, V.; Butyrina, T.; Vasil'eva, E.; Danilov, F. *Turk. J. Chem.* **2014**, *38*, 50–55.
12. Danilov, F. I.; Protsenko, V. S.; Butyrina, T. E.; Vasil'eva, E. A.; Baskevich, A. S. *Prot. Met.* **2006**, *42*, 560–569.
13. Akiyama, T.; Kobayashi, S.; Ki, J.; Ohgai, T.; Fukushima, H. *J. Appl. Electrochem.* **2000**, *30*, 817–822.
14. Janssen, L. J. J.; Hoogland, J. G. *Electrochim. Acta* **1970**, *15*, 1013–1023.
15. Protsenko, V. S.; Danilov, F. I. *Russ. J. Electrochem.* **2005**, *41*, 108–112.
16. Wei, D.; Ma, Q.; Guan, Y.; Hu, F.; Zheng, A.; Zhang, X.; Teng, Z.; Jiang, H. *Mater. Sci. Eng. C* **2009**, *29*, 1776–1780.
17. Protsenko, V.; Danilov, F. *Electrochim. Acta* **2009**, *54*, 5666–5672.
18. Danilov, F. I.; Protsenko, V. S. *Prot. Met.* **2001**, *37*, 223–228.
19. Vetter, K. *Electrochemical Kinetics*; Academic Press: New York, NY, USA, 1967.
20. Frolov, Yu. G. *Course of Colloid Chemistry. Surface Phenomena and Dispersed Systems*; Khimiya: Moscow, 1988 (in Russian).
21. Plieth, W. *J. Solid State Electrochem.* **2011**, *15*, 1417–1423.